ACI STRUCTURAL JOURNAL TECHNICAL PAPER

Title no. 85-S11

Strength of Slab-Column Edge Connections

by Jack P. Moehle

Selected experimental data on the strength of slab-column edge connections transferring moment perpendicular to the edge are reviewed. The eccentric shear stress model that forms that basis of design according to the ACI Building Code (ACI 318-83) is found not to correlate well with the data. An alternate analysis model is proposed, assuming that moment transfer strength is limited solely by available flexural reinforcement within an effective transfer width and is not influenced by connection shear. The proposed model correlates well with the experimental data and simplifies the design and analysis process.

Keywords: columns (supports); concrete slabs; connections; flat concrete plates; moments; reinforced concrete; shear strength; **strength;** structural design.

Methods for computing strength of slab-column edge connections tend to be filled with complications that are inconsistent with the approximate nature of the computed strength. This inconsistency has been a source of irritation for the engineer who must contend with the complicated and restrictive strength analysis procedures of current codes (eg., ACI 318-83[1]). As will be demonstrated in this paper, commonly accepted strength analysis methods are excessively inaccurate and complex for the edge connection transferring moment perpendicular to the slab edge. A new strength model will be developed correlating well with observed experimental trends and simplifying design.

The paper begins with a summary of data obtained from numerous experiments on slab-column edge connections transferring shear and moment normal to the slab edge. The strength analysis model embodied in the current ACI Building Code (ACI 318-83)[1] is described and compared with the experimental data. A new approach is derived and verified by the experiments. Applications in design are also described.

REVIEW OF EXPERIMENTAL DATA

Table 1 summarizes key parameters of 27 experiments in which slab-column edge connections were tested to failure. The list is not exhaustive but includes specimens encompassing a broad range of connection configurations and test methods. Details of the tests are given in References 2 through 9. A review of most of these data and an enlightening analytical treatment of the test results are in the report by Alexander and Simmonds.[2]

For all test specimens included in this study, the outer face of the columns was flush with the slab edge and extended both above and below the slab (Fig. 1). With the exception of the specimens tested by Regan[6] and Scavuzzo,[7] all were isolated single column-slab connections, as shown in Fig. 1(a). The specimens tested by Regan comprised a slab spanning two edge connections, as illustrated in Fig. 1(b). The Scavuzzo specimen comprised both an interior and exterior connection, as shown in Fig. 1(c). None of the connections had slab shear reinforcement or edge beams, and none transferred moment parallel to the slab edge. The specimens tested by Hawkins, Wong, and Yang[4] were subjected to inelastic load reversals simulating earthquake effects.

To avoid difficulties in computing slab unit moment strengths in the vicinity of the column, only connections having relatively uniform distributions of top slab reinforcement in the region approximately 1.5 column widths on either side of the column are included in Table 1. Connections that had a top slab steel ratio less than 0.0025 are excluded because they are considered atypical. All connections had a bottom mat of slab reinforcement in the vincinity of the column.

Based on experimental observations from these tests, the following brief discussion of behavior is presented. More detailed presentations are made elsewhere.[2-9]

For most slab-column edge connections, the failure is described as a punching failure in which the column

Received Dec. 1, 1986, and reviewed under Institute publication policies.
Copyright © 1988. American Concrete Institute. All rights reserved, including the making of copies unless permission is obtained from the copyright proprietors. Pertinent discussion will be published in the November-December 1988 *ACI Structural Journal* if received by July 1, 1988.

*ACI member **Jack P. Moehle** is an associate professor of civil engineering at the University of California at Berkeley. He received the BS, MS, and PhD (1980) degrees from the University of Illinois at Urbana-Champaign. He is a member of ACI-ASCE Committees 352, Joints and Connections, and 442, Response to Lateral Forces. He is active in research on behavior and design of flat-slab structures subjected to vertical and lateral loads.*

and a portion of the slab adjacent to the column push through the surrounding slab. A typical failure surface and accompanying crack pattern are shown in Fig. 2. Similar to results observed for interior connections,[10] punching failure is generally preceded by yield of slab reinforcement near the column. For connections with significant moment transfer at failure, torsional cracks and apparent torsional yield lines form in the slab adjacent to the column side faces (Fig. 2). Where the slab edge has sufficient torisonal strength, as in the extreme case where an edge beam is present, the slab may develop flexural yield lines across the full transverse width of the slab prior to final failure.[11]

Test data indicate that shear and moment strengths of edge connections are influenced by slab thickness, column dimensions, materials, and slab-steel ratios in much the same manner as these variables influence strength of interior connections. However, unlike interior connections, there appears to be less pronounced interaction between shear and moment at the connection. This phenomenon is illustrated by the results obtained in the series of tests by Stamenkovic and Chapman[8] and a subset of the test series of Zaghlool [Specimens Z-V(1), Z-V(5), and Z-V(6)].[9] In each of these two series of tests, connection geometry, reinforcement, and material properties were kept nominally identical with minor variations in concrete strength (Table 1). The main variable in each series was the ratio between connection shear and moment at failure.

Fig. 3 shows the variation of moment and shear at failure for these tests. The resisting moment is normalized to the moment strength M_o measured in the absence of shear, and the resisting shear is normalized to the shear strength V_o measured in the absence of moment. No correction is made for variation of concrete strength. The trend of the data supports the contention that there is no significant interaction between shear and moment strengths; failure occurs effectively when the moment reaches M_o or the shear reaches V_o, whichever occurs first. Thus, a simple bilinear interaction diagram, such as shown by the broken lines in Fig. 3, is appropriate.

For the connections analyzed in Fig. 3, strengths for various combinations of shear and moment can be computed according to the eccentric shear stress model that is the basis of the ACI Building Code design specification.[1] (Details of the analytical model are presented later in the paper.) The interaction diagrams re-

Table 1 — Test specimen data

Researcher	Mark	h, in.	c_1, in.	c_2, in.	d_1, in.	d_{av}, in.	ρ_c, %	ρ_{l1}, %	ρ_{l2}, %	f'_c, psi	f_y, ksi	V_u, kip	M_u, kip-in.
Col. 1	Col. 2	Col. 3	Col. 4	Col. 5	Col. 6	Col. 7	Col. 8	Col. 9	Col. 10	Col. 11	Col. 12	Col. 13	Col. 14
Stamenkovic and Chapman[8]	V/E/1	3.00	5.00	5.00	2.36	2.20	1.09	1.09	1.09	4230	71.9	16.8	0
	C/E/1	3.00	5.00	5.00	2.36	2.20	1.09	1.09	1.39	4570	65.0	16.5	49.5
	C/E/2	3.00	5.00	5.00	2.36	2.20	1.09	1.09	1.39	4780	71.9	12.3	81.2
	C/E/3	3.00	5.00	5.00	2.36	2.20	1.09	1.09	1.39	4930	71.9	5.6	89.0
	C/E/4	3.00	5.00	5.00	2.36	2.20	1.09	1.09	1.39	4030	71.9	2.46	78.2
	M/E/2	3.00	5.00	5.00	2.36	2.20	1.09	1.09	1.39	3870	71.9	0.00	74.0
Kane[5]	K-1	2.00	3.94	2.68	1.73	1.61	0.99	0.99	1.38	4380	69.6	5.40	21.1
	K-3	1.89	4.49	2.95	1.62	1.5	1.12	1.12	1.31	5980	69.6	5.64	21.9
Zaghlool[9]	Z-1V(1)	6.00	7.00	7.00	5.00	4.75	2.29	1.18	2.41	3970	69.0	27.5	398
	Z-V(1)	6.00	10.5	10.5	5.00	4.75	1.52	1.18	1.60	4980	68.7	48.4	749
	Z-V(2)	6.00	10.5	10.5	5.00	4.75	1.72	1.49	2.00	5870	68.7	55.5	828
	Z-V(3)	6.00	10.5	10.5	4.91	4.63	1.75	1.86	1.65	5620	68.9	60.3	917
	Z-V(4)	6.00	10.5	10.5	5.00	4.75	1.52	1.18	1.60	5080	63.4	0.00	720
	Z-V(5)	6.00	10.5	10.5	5.00	4.75	1.52	1.18	1.60	5100	69.0	62.8	0
	Z-V(6)	6.00	10.5	10.5	5.00	4.75	1.52	1.18	1.60	4540	69.1	26.3	780
	Z-VI(1)	6.00	14.0	14.0	5.00	4.75	1.14	1.18	2.41	3770	69.0	59.6	946
Regan[6]	SE1	4.92	11.8	7.87	4.10	3.86	1.08	1.08	1.15	5150	69.6	44.5	350
	SE4	4.92	7.87	11.8	4.10	3.86	1.08	1.08	1.15	3860	69.6	34.1	270
	SE7	4.92	7.87	11.8	4.06	3.86	1.08	0.52	1.15	5770	71.1	29.0	281
	SE9	4.92	9.84	9.84	4.10	3.86	0.54	0.54	0.92	6080	69.6	27.7	316
	SE10	4.92	9.84	9.84	4.10	3.86	0.54	0.54	0.92	5960	69.6	25.6	319
	SE11	4.92	9.84	9.84	4.10	3.86	0.54	0.54	0.92	7470	69.6	31.0	350
Scavuzzo[7]	S1	2.50	6.00	4.00	2.06	1.95	0.65	0.78	1.03	5530	55.0	7.22	41.2
Hawkins, Wong, and Yang[4]	E1	6.50	12.0	12.0	5.44	5.13	0.76	0.76	0.76	3270	67.1	14.3	599
	E2	7.00	16.0	16.0	5.88	5.50	1.07	1.07	1.07	4280	61.7	18.7	1330
	E3	7.00	19.5	8.00	5.88	5.50	1.87	1.25	1.54	3280	64.9	18.5	1120
Hanson and Hanson[3]	D15	3.00	6.00	6.00	2.44	2.25	1.50	1.50	1.63	4510	53.0	2.71	93.0
Minimum		1.89	3.94	2.68			0.54	0.52	0.76	3270	53.0		
Maximum		7.00	19.5	16.0			2.29	1.86	2.41	7470	71.9		
Mean		4.64	8.85	8.39			1.19	1.06	1.40	4846	67.8		

Note: 1 in. = 25.4 mm; 1 psi = 6895 Pa; 1 kip = 4.448 kN; 1 kip-in. = 113 Nm.

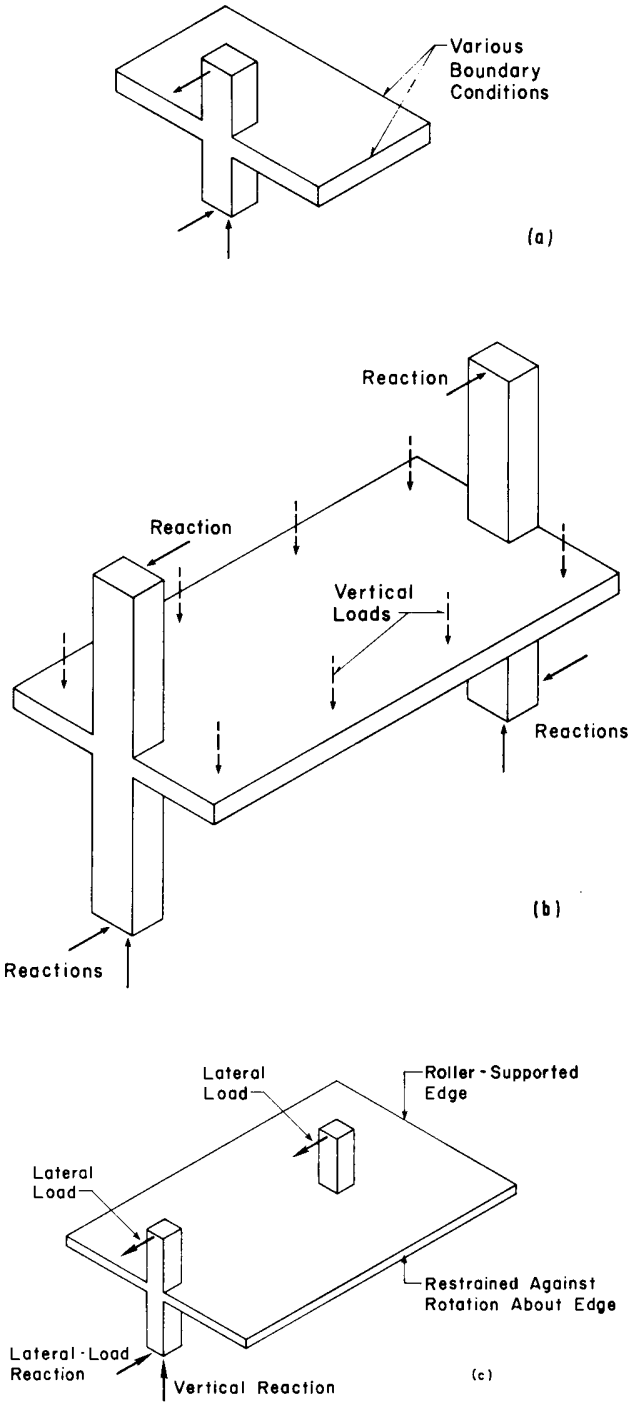

Fig. 1—Test specimen configurations — (a) Isolated connection specimens; (b) Regan test specimens; and (c) Scavuzzo test specimens

sulting from the ACI Code procedure are plotted with solid lines in Fig. 3, with computed shear and moment strengths normalized to the measured pure shear and moment strengths, respectively. The relatively complex computed interaction is neither verified nor disproved by the measured data but is almost surely unjustified in light of the more simple bilinear interaction displayed by the data.

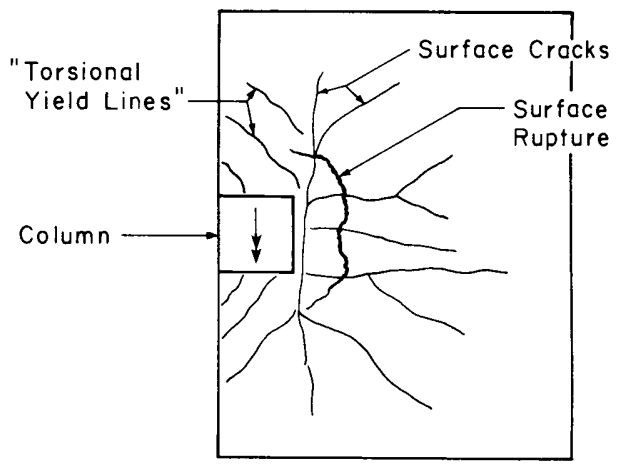

Fig. 2—Typical damage at failure

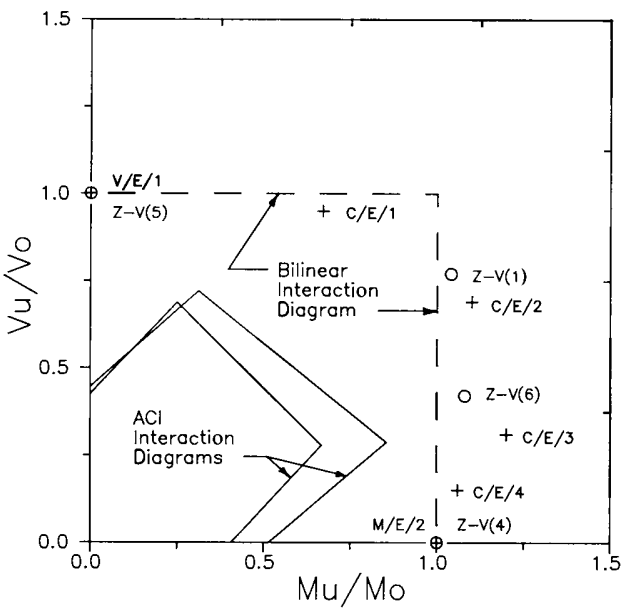

Fig. 3—Interaction between shear and moment

Further discussions of the eccentric shear stress model and comparisons with selected data are presented next.

COMPARISON OF THE ECCENTRIC SHEAR STRESS MODEL WITH EXPERIMENTAL DATA

The strength analysis method described in the ACI Building Code[1] for slab-column edge connections was developed from ideas presented originally by Di Stasio and Van Buren.[12] The present form of the method can be attributed essentially to the work of Hanson and Hanson[3] and is based primarily on data obtained from interior connection tests. The method is reasonably straightforward and has been verified for interior connections. It is cumbersome and largely unverified for edge connections.

The analytical model envisions a linear variation of slab shear stress on a slab critical section, the stresses being related to the shear and a prescribed proportion

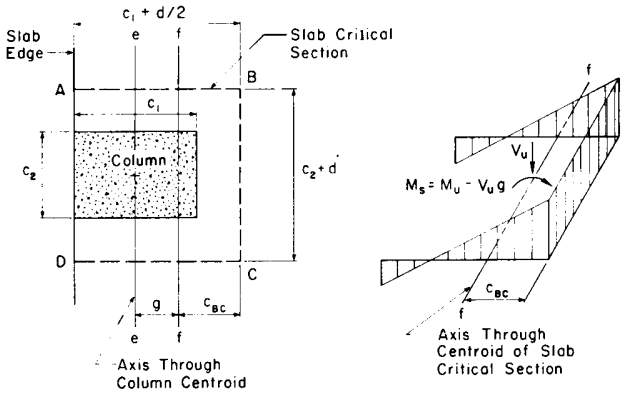

Fig. 4—Definition of critical section and shear stresses according to ACI Building Code

of the moment transferred to the connection (Fig. 4). Shear failure is presumed to occur when the maximum shear stress reaches a limiting value v_c given by Eq. (1)

$$v_c = (2 + 4/\beta_c)\sqrt{f'_c} \text{ but not greater than } 4\sqrt{f'_c} \quad (1)$$

in which v_c is given in psi units, β_c = ratio between long and short cross-sectional dimensions of the column, and f'_c = concrete compressive strength in psi units. In MPa units, Eq. (1) is rewritten as Eq. (1a)

$$v_c = 0.17(1 + 2/\beta_c)\sqrt{f'_c} \quad (1a)$$
$$\text{but not greater than } \sqrt{.33 f'_c}$$

Slab flexural steel is required within a width $c_2 + 3h$ to resist connection moments not resisted by slab-shear stresses. Thus, connection moment transfer strength (with moment defined at the centroid of the slab critical section) is calculated to be limited by the most critical of three moment values: M_{vBC}, corresponding to reaching the limiting shear stress v_c on the inner face BC of the slab critical section; M_{vAD}, corresponding to reaching the limiting shear stress v_c on the outer face AD of the slab critical section; and M_f, corresponding to reaching the limiting flexural strength of slab reinforcement within the prescribed transfer width. Details of the calculation procedure can be found elsewhere.[13,14]

The analytical model can be gaged for accuracy using the data summarized in Table 1. Moments M_s acting at the centroid of the slab critical section at failure were calculated for each specimen as $M_u - V_u g$, in which g is the distance between centroids of the slab critical section and the column cross section. Values of M_s are in Column 4 of Table 2. Given values of moment M_s and shear V_u, shear stresses on inner and outer faces of the slab critical section can be computed ac-

Table 2 — Strength ratios according to the eccentric shear stress model of the ACI Building Code

Researcher	Mark	V_u, kip	M_s, kip-in.	V_u/V_o	v_{BC}/v_c	v_{AD}/v_c	M_s/M_f	Max.*
Col. 1	Col. 2	Col. 3	Col. 4	Col. 5	Col. 6	Col. 7	Col. 8	Col. 9
Stamenkovic and Chapman[8]	V/E/1	16.8	−28.3	1.51	1.09	2.44	−.32	2.44
	C/E/1	16.5	21.8	1.43	1.74	0.74	0.27	1.74
	C/E/2	12.3	60.5	1.04	1.90	0.82	0.69	1.90
	C/E/3	5.60	79.6	0.47	1.57	1.94	0.90	1.94
	C/E/4	2.46	74.1	0.23	1.36	2.25	0.86	2.25
	M/E/2	0.00	74.0	0.00	1.16	2.53	0.86	2.53
Kane[9]	K-1	5.40	14.9	0.92	1.57	0.31	0.54	1.57
	K-3	5.64	15.4	0.81	1.36	0.19	0.55	1.36
Zaghlool[9]	Z-1V(1)	27.5	316	0.75	1.61	1.17	0.46	1.61
	Z-V(1)	48.4	576	0.88	1.70	0.91	0.69	1.70
	Z-V(2)	55.0	629	0.93	1.76	0.88	0.60	1.76
	Z-V(3)	60.3	703	1.07	2.05	1.08	0.57	2.05
	Z-V(4)	0.00	720	0.00	1.02	2.22	0.93	2.22
	Z-V(5)	62.8	−225	1.13	0.81	1.82	−.27	1.82
	Z-V(6)	26.3	686	0.50	1.53	1.74	0.83	1.74
	Z-VI(1)	59.6	698	0.99	1.74	0.61	0.76	1.74
Regan[6]	SE1	44.5	216	1.02	1.49	0.17	0.48	1.49
	SE4	34.1	163	1.01	1.41	0.05	0.36	1.41
	SE7	29.0	190	0.70	1.09	0.31	0.82	1.09
	SE9	27.7	229	0.62	1.07	0.35	0.94	1.07
	SE10	25.6	239	0.58	1.05	0.45	0.98	1.05
	SE11	31.0	253	0.62	1.07	0.34	1.03	1.07
Scavuzzo[7]	S1	7.22	30.2	0.63	1.10	0.26	0.88	1.10
Hawkins, Wong, and Yang[4]	E1	14.4	542	0.27	0.97	1.26	0.78	1.26
	E2	18.7	1242	0.22	1.04	1.55	1.00	1.55
	E3	18.5	1043	0.25	1.27	1.38	0.83	1.38
Hanson and Hanson[3]	D15	2.71	87.9	0.20	1.14	1.84	0.85	1.84
Minimum				0.00				1.05
Maximum				1.51				2.53
Mean				0.70				1.65
Coefficient of variation				0.57				0.25

*Maximum of values in Columns 6 through 8.
Note: 1 kip = 4.448 kN; 1 kip-in. = 113 Nm.

cording to the eccentric shear stress model. Ratios between the computed stresses and the nominal shear stress capacity v_c [given by Eq. (1)] are tabulated in Columns 6 and 7 of Table 2. In addition, ratios between applied moment M_s and computed connection strength limited by flexural reinforcement M_f are tabulated in Column 8 of Table 2. For each specimen, the largest of the three strength ratios in Columns 6 through 8 is the critical ratio between measured and computed strength because failure is predicted when that quantity reaches a value of unity. Column 9 of Table 2 presents the maximum of the three values in Columns 6 through 8.

Range, mean, and coefficient of variation for the critical strength ratios (Column 9) are presented at the bottom of Table 2. The individual values from Column 9 are plotted as the coordinates in Fig. 5. The horizontal axis in Fig. 5 is the ratio V_u/V_o, in which V_o is a calculated shear strength in the absence of moment transfer,[1] as given by Eq. (2)

$$V_o = v_c A_{cs} \quad (2)$$

in which A_{cs} = area of a slab critical section located a distance $d/2$ from the column faces and having depth

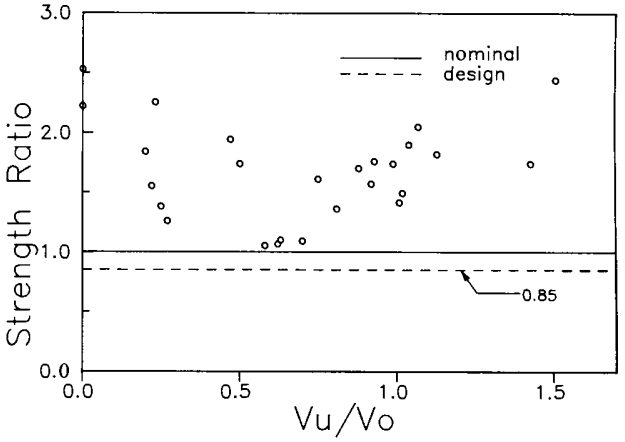

Fig. 5—Ratio between measured strength and strength computed according to the ACI Building Code

equal to d, d = average slab effective depth, and v_c is given by Eq. (1).

Analysis of the data in Table 2 reveals that calculated strength is governed by limiting shear stresses on the slab critical section rather than flexural yield for all of the test specimens. Calculated strengths are in all cases conservative, with ratios between measured and calculated strengths ranging from 1.04 to 2.53, and

Table 3 — Strength ratios based on reduced values of γ_v

			$1/2\gamma_v$			$\gamma_v = 0$		
Researcher	Mark	V_u/V_o	v_{BC}/v_c	v_{AD}/v_c	M_s/M_f	Max.*	M_s/M_f	Max.†
Col. 1	Col. 2	Col. 3	Col. 4	Col. 5	Col. 6	Col. 7	Col. 8	Col. 9
Stamenkovic and Chapman[8]	V/E/1	1.51	1.30	1.98	**−0.42**	1.98	− .52	1.51
	C/E/1	1.43	1.58	1.08	0.36	1.58	0.44	1.43
	C/E/2	1.04	1.47	0.11	0.89	1.47	1.10	1.10
	C/E/3	0.47	1.02	0.74	1.17	1.17	1.44	1.44
	C/E/4	0.23	0.80	1.01	1.12	1.12	1.37	1.37
	M/E/2	0.00	0.58	1.26	1.12	1.26	1.38	1.38
Kane[5]	K-1	0.92	1.24	0.30	0.73	1.24	0.92	0.93
	K-3	0.81	1.08	0.31	0.75	1.08	0.95	0.95
Zaghlool[9]	Z-1V(1)	0.75	1.18	0.21	0.60	1.18	0.73	0.76
	Z-V(1)	0.88	1.29	0.02	0.91	1.29	1.11	1.11
	Z-V(2)	0.93	1.34	0.03	0.79	1.34	0.97	0.97
	Z-V(3)	1.07	1.56	0.01	0.75	1.56	0.92	1.08
	Z-V(4)	0.00	0.51	1.11	1.21	1.21	1.49	1.49
	Z-V(5)	1.13	0.97	1.48	−0.35	1.48	−0.43	1.14
	Z-V(6)	0.50	1.01	0.62	1.09	1.09	1.34	1.34
	Z-VI(1)	0.99	1.37	0.19	0.99	1.37	1.22	1.22
Regan[6]	SE1	1.02	1.26	0.60	0.65	1.26	0.82	1.03
	SE4	1.01	1.21	0.48	0.45	1.21	0.55	1.01
	SE7	0.70	0.90	0.20	1.03	1.03	1.24	1.24
	SE9	0.62	0.84	0.13	1.24	1.24	1.52	1.52
	SE10	0.58	0.81	0.07	1.29	1.29	1.59	1.59
	SE11	0.62	0.85	0.14	1.35	1.35	1.67	1.67
Scavuzzo[7]	S1	0.63	0.86	0.18	1.19	1.19	1.50	1.50
Hawkins, Wong, and Yang[4]	E1	0.27	0.62	0.50	1.02	1.02	1.25	1.25
	E2	0.22	0.63	0.66	1.31	1.31	1.62	1.62
	E3	0.25	0.76	0.56	1.18	1.18	1.53	1.53
Hanson and Hanson[3]	D15	0.20	0.67	0.82	1.12	1.12	1.38	1.38
Minimum		0.00				1.02		0.76
Maximum		1.51				1.98		1.67
Mean		0.70				1.28		1.28
Coefficient of variation		0.57				0.20		0.19

*Maximum of values in Columns 4 through 6.
†Maximum of values in Columns 3 and 8.

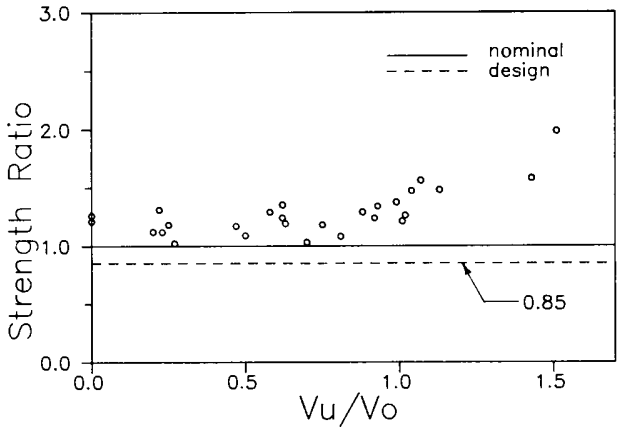

Fig. 6—Ratio between measured strength and strength computed according to the ACI Building Code using half the specified value of γ_v

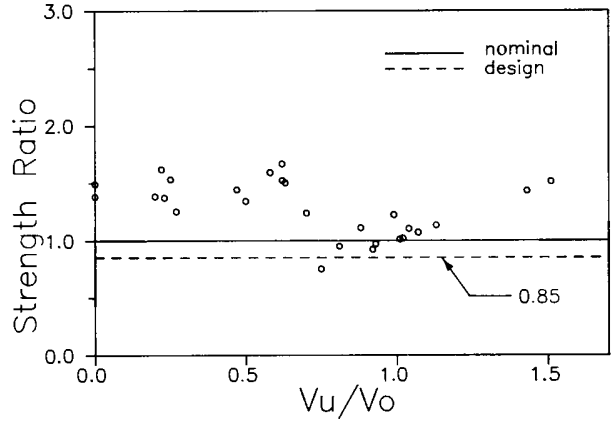

Fig. 7—Ratio between measured strength and strength computed according to the ACI Building Code with γ_v = 0

having a mean of 1.65 and a coefficient of variation of 0.25.

The overconservative and scattered trend of the data presented in Table 2 and Fig. 5 occurs in part because the analytical model assumes a significant interaction between shear and moment, whereas the trends of available data do not show such an interaction (Fig. 3). In support of this claim, Table 3 and Fig. 6 and 7 present strength ratios, analogous to those in Fig. 5, but with reductions in the proportion of moment carried by eccentric shear stresses. In Columns 4 through 7 of Table 3 and in Fig. 6, the proportion of moment assumed to be carried by eccentric shear is half that prescribed in the ACI Building Code, and the proportion carried by flexural steel is increased correspondingly. In Columns 8 and 9 of Table 3 and in Fig. 7, calculated strengths assume all of the connection moment is carried by flexural steel and none by eccentric shear stresses.

The data in Fig. 6 and 7 show that improved correlations between measured and calculated strengths can be obtained assuming reduced interactions between

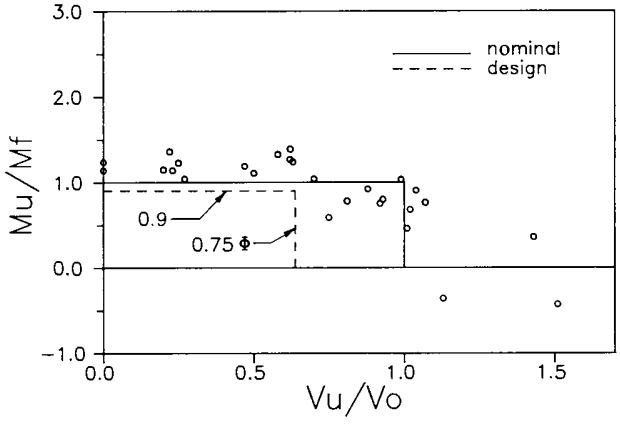

Fig. 8—Ratio between measured and calculated moment transfer strengths using effective transfer width of $c_2 + 4h$

shear and moment. Several of the strength ratios in Fig. 7 fall below a value of unity for ratios V_u/V_o, exceeding approximately 0.75, suggesting that it may be overly simplistic to ignore completely shear and moment interactions for connections carrying relatively large vertical shears. However, current design algorithms[1,15] indirectly eliminate such heavily loaded connections in actual construction. Any new design method that proposes to ignore shear and moment interaction (as in Fig. 7) should likewise preclude the possibility of excessive connection shears. Before discussing details of such a design method, aspects of the moment transfer strength will be discussed in greater detail.

EFFECTIVE MOMENT TRANSFER WIDTH

The preceding analysis supports a general conclusion that moment transfer strength normal to the slab edge is independent of the direct shear on the connection. More specifically, the analysis suggests that moment transfer strength is equal to the flexural strength of slab reinforcement within an effective transfer width. The strength ratios in Fig. 7 were computed by assuming a transfer width equal to $c_2 + 3h$ as specified in the ACI Building Code, in which c_2 = column width parallel to the slab edge and h = the slab thickness. The following discussion evaluates alternate effective transfer widths.

The data in Fig. 7, for ratios V_u/V_o less than 0.75, are consistently conservative, suggesting that the assumed transfer width equal to $c_2 + 3h$ is unnecessarily narrow. A simple fix is to increase the effective transfer width to $c_2 + 4h$. Fig. 8 plots results with this new effective width. The vertical axis in this figure is the ratio between measured moment strength (at centroid of the slab critical section) and computed flexural strength of a section of slab having width $c_2 + 4h$. (Note that the entire moment is assumed to be resisted in flexure by steel within $c_2 + 4h$, in contrast with the ACI Building Code procedure in which only a portion of the connection moment is carried by flexure.) For V_u/V_o ratios less than 0.75, correlation is improved using the increased effective width.

Alternate effective widths can be derived by consideration of apparent yield-line patterns at an edge connection at failure. As sketched in Fig. 2 and idealized in Fig. 9, failure of a connection transferring normal moment involves development of apparent flexural and torsional yield lines forming around the connection. The moment transfer strength can be approximated as the total flexural strength of reinforcement normal to the slab edge and crossing the slab yield lines. To determine the moment strength, the projection of the torsional yield lines must first be estimated.

The projection of the torsional yield lines (Fig. 9) is approximated using concepts of diagonal compression theory.[16] As illustrated in Fig. 9(b), diagonal compression struts are assumed to form parallel to the torsional yield lines at the side faces of the column. The longitudinal and transverse components of the compression force in the struts are balanced by tensile forces developed in the longitudinal and transverse top reinforcements, respectively, crossing the yield line. Hence, the total force N_t, in the transverse top reinforcement, and total force N_l, in the longitudinal top reinforcement, are given by

$$N_t = N_d \cos \alpha \quad \text{and} \quad N_l = N_d \sin \alpha \tag{3}$$

Eq. (4) is derived from Eq. (3)

$$N_l/N_t = \tan \alpha \tag{4}$$

Assuming that all reinforcement crossing the yield lines is stressed to yield, the quantities N_t and N_l can be written in terms of transverse and longitudinal top reinforcement, as given in Eq. (5)

$$N_t = \rho_t f_y c_1 d \quad \text{and} \quad N_l = \rho_l f_y c_t d \tag{5}$$

in which ρ_t and ρ_l = reinforcement ratios for the transverse and longitudinal top reinforcement, respectively, and f_y = reinforcement yield stress. Substituting Eq. (5) into Eq. (4) and recognizing that $\tan \alpha = c_1/c_t$, Eq. (6) can be written for the projection c_t of the torsional yield line

$$c_t = c_1 \sqrt{\rho_t/\rho_l} \tag{6}$$

The effective transfer width based on the preceding model is equal to $c_2 + 2c_t$ [Fig. 9(a)]. An expression having the same implication as Eq. (6) has been presented by Regan and Braestrup.[17]

Ratios between measured moment strength (at centroid of slab critical section) and strength computed with this effective transfer width are in Fig. 10 and in Column 8 of Table 4. Correlation between computed and measured strengths is improved by comparison with Fig. 9, but the improvement is not significant.

Computed values of the angle α (Fig. 11) do not deviate substantially from a value of 45 deg. This observation suggests that the strength analysis can be simplified by taking α equal to 45 deg, resulting in an effective transfer width equal to $c_2 + 2c_1$. Strength ratios computed with this simpler effective width are tabulated in Columns 10 and 11 of Table 4 and are plotted in Fig. 12. The degree of accuracy in computed

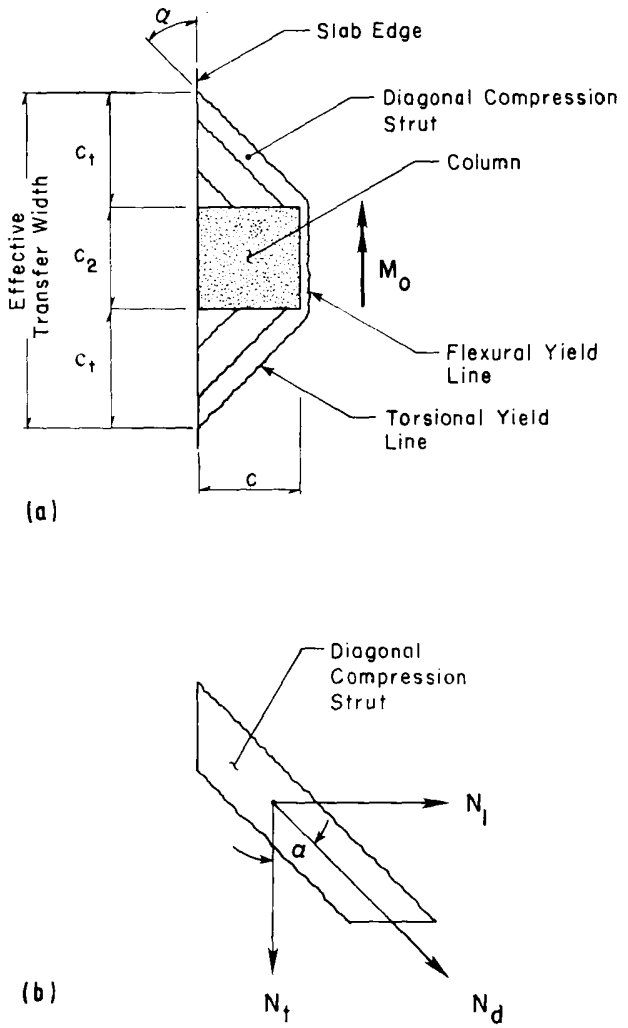

Fig. 9—Illustration of diagonal compression struts at edge connection

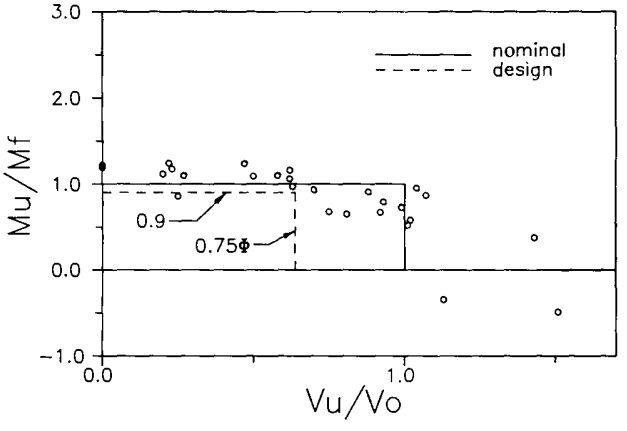

Fig. 10—Ratio between measured and calculated moment transfer strengths using effective transfer width from computed values of α

Table 4 — Strength ratios based on various effective transfer widths

Researcher	Mark	V_u/V_o	Transfer width $c_2 + 3h$ M_s/M_f	$c_2 + 3h$ Max.*	$c_2 + 4h$ M_s/M_f	$c_2 + 4h$ Max.†	$c_2 + 2c_1$ M_s/M_f	$c_2 + 2c_1$ Max.‡	$c_2 + 2c_1$ M_s/M_f	$c_2 + 2c_1$ Max.§
Col. 1	Col. 2	Col. 3	Col. 4	Col. 5	Col. 6	Col. 7	Col. 8	Col. 9	Col. 10	Col. 11
Stamenkovic and Chapman[8]	V/E/1	1.51	−0.52	1.51	−0.43	1.51	−0.49	1.51	−0.48	1.51
	C/E/1	1.43	0.44	1.43	0.36	1.43	0.38	1.43	0.41	1.43
	C/E/2	1.04	1.10	1.10	0.91	1.04	0.95	1.04	1.03	1.04
	C/E/3	0.47	1.44	1.44	1.19	1.19	1.24	1.24	1.35	1.35
	C/E/4	0.23	1.37	1.37	1.14	1.14	1.18	1.18	1.29	1.29
	M/E/2	0.00	1.38	1.38	1.14	1.14	1.19	1.19	1.29	1.29
Kane[5]	K-1	0.92	0.92	0.92	0.75	0.92	0.67	0.92	0.76	0.92
	K-3	0.81	0.95	0.95	0.78	0.81	0.65	0.81	0.69	0.81
Zaghlool[9]	Z-1V(1)	0.75	0.73	0.75	0.59	0.75	0.68	0.75	0.88	0.88
	Z-V(1)	0.88	1.11	1.11	0.92	0.88	0.91	0.91	1.01	1.01
	Z-V(2)	0.93	0.97	0.97	0.80	0.93	0.79	0.93	0.88	0.93
	Z-V(3)	1.07	0.92	1.07	0.76	1.07	0.87	1.07	0.84	1.07
	Z-V(4)	0.00	1.49	1.49	1.24	1.24	1.22	1.22	1.35	1.35
	Z-V(5)	1.13	−0.43	1.13	−0.36	1.13	−0.35	1.13	−0.39	1.13
	Z-V(6)	0.50	1.34	1.34	1.11	1.11	1.09	1.09	1.21	1.21
	Z-VI(1)	0.99	1.22	1.22	1.03	1.03	0.73	0.99	0.94	0.99
Regan[6]	SE1	1.02	0.82	1.02	0.68	1.02	0.58	1.02	0.59	1.02
	SE4	1.01	0.55	1.01	0.46	1.01	0.52	1.01	0.53	1.01
	SE7	0.70	1.24	1.24	1.04	1.04	0.93	0.93	1.20	1.20
	SE9	0.62	1.52	1.52	1.27	1.27	1.06	1.06	1.27	1.27
	SE10	0.58	1.59	1.59	1.33	1.33	1.10	1.10	1.33	1.33
	SE11	0.62	1.67	1.67	1.39	1.39	1.16	1.16	1.39	1.39
Scavuzzo[7]	S1	0.63	1.50	1.50	1.24	1.24	0.97	0.97	1.09	1.09
Hawkins, Wong, and Yang[4]	E1	0.27	1.25	1.25	1.04	1.04	1.10	1.10	1.10	1.10
	E2	0.22	1.62	1.62	1.36	1.36	1.25	1.25	1.25	1.25
	E3	0.25	1.53	1.53	1.23	1.23	0.86	0.86	0.94	0.94
Hanson and Hanson[3]	D15	0.20	1.38	1.38	1.15	1.15	1.12	1.12	1.15	1.15
Minimum				0.76		0.75		0.75		0.81
Maximum				1.67		1.51		1.51		1.51
Mean				1.28		1.13		1.07		1.15
Coefficient of variation				0.19		0.17		0.16		0.16

*Maximum of values in Columns 3 and 4.
†Maximum of values in Columns 3 and 6.
‡Maximum of values in Columns 3 and 8.
§Maximum of values in Columns 3 and 10.

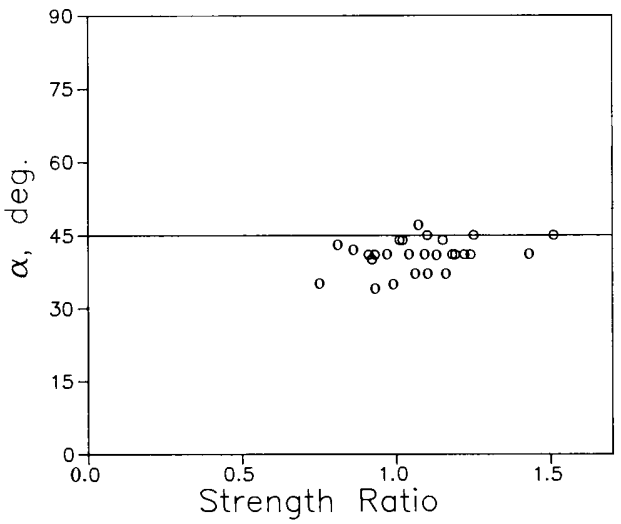

Fig. 11—Variation of calculated values of α with calculated strength ratios (Column 9 of Table 4)

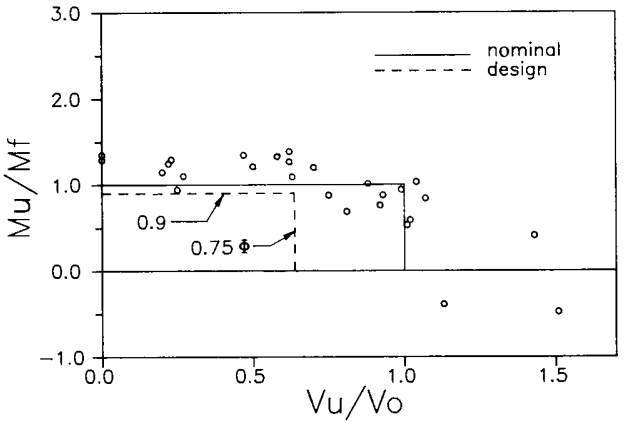

Fig. 12—Ratio between measured and calculated moment transfer strengths assuming α = 45 deg

strengths is not inordinately sacrificed using this simplifying assumption.

A recent paper[18] on corner connections indicates that if the column does not extend above the floor slab, the slab yield lines may pass over the column, rather than around the column as implied in the present study. In this case, the slab effective transfer width is reduced below that indicated in the preceding discussion. This phenomenon should be considered, for example, at roof connections where column stubs do not protrude above the floor slab.

DESIGN APPLICATIONS

The preceding analysis of experimental data suggests that if connection shear is kept to a reasonable value, there is effectively no interaction between shear and moment effects. Moment transfer strength is related to

the flexural strength of slab reinforcement within an effective slab width and is not affected by connection shear transfer. Shear strength is affected by size of the connection and concrete strength and is not affected by connection moment transfer.

As has been noted repeatedly, shear-moment interaction can be ignored only if the total connection shear is less than approximately 75 percent of the pure shear strength V_o, where V_o is given by Eq. (2). Assuming a nominal shear stress capacity $v_c = 4\sqrt{f'_c}$ psi ($0.33\sqrt{f'_c}$ MPa), and applying a strength reduction factor of $\phi = 0.85$, the maximum nominal shear stress that should be allowed on the slab critical section, due to direct shear transfer only, is approximately $0.75\phi 4\sqrt{f'_c}$ psi $= \phi 3\sqrt{f'_c}$ psi $\approx 2.5\sqrt{f'_c}$ psi ($0.75\phi 0.33\sqrt{f'_c}$ MPa $= \phi 0.25\sqrt{f'_c}$ MPa $\approx 0.2 f'_c$ MPa). This stress limit is based solely on strength considerations. It is roughly consistent with recommendations made previously by Hawkins and Mitchell,[18] who observed that allowable shear stresses for interior connections should be reduced if general yield of the slab reinforcement is anticipated. This limiting shear stress will result in connection sizes not significantly different from those occurring in current design practice.[15]

All connections analyzed in this paper had a continuous mat of bottom slab reinforcement. It is not known how this influenced the findings reported here. In view of this uncertainty and in view of the proven capacity for bottom reinforcement to delay progressive collapse,[19] it is recommended that connections be designed with a continuous mat of bottom reinforcement in the connection region. At least temperature and shrinkage reinforcement around the connection, and continuity steel satisfying the intent of Reference 19, should be provided.

Based on analysis of data presented in this paper, an appropriate design procedure is as follows:

1. A frame analysis is conducted to determine required ultimate connection strengths in shear and moment acting at the centroid of the column cross section. Consistent with current design methods for slab connections,[1] the connection design moment is taken at the centroid of the slab critical section rather than at the centroid of the column cross section.

2. The connection is sized to insure that ultimate shear does not exceed the value $0.75\phi v_c A_{cs}$, in which $\phi = 0.85$, v_c is given by Eq. (1) in psi units [or Eq. (1a) in MPa units], and A_{cs} = area of the slab critical section located a distance $d/2$ from the column face.

3. Sufficient flexural reinforcement is placed within the effective transfer width shown in Fig. 9(a) to resist all of the required connection moment acting at the centroid of the slab critical section. Reliable flexural strength is calculated following the usual assumptions,[10] with capacity reduction factor $\phi = 0.9$. The effective transfer width can be taken equal to $c_2 + 2c_t$, where c_t is equal to c_1, but not to exceed the distance from the inner face of the column to the slab edge. (More refined estimates of c_t are not warranted currently.) Because some flexural ductility is required to fully develop the yield lines around the connection [Fig. 9(a)], it is recommended that the slab-steel ratio should not exceed $0.5\rho_b$, where ρ_b is the balanced steel ratio.

SUMMARY AND CONCLUSIONS

Strength and behavior of reinforced concrete slab-column edge connections transferring shear and moment normal to the slab edge are analyzed. Data from 27 experiments conducted by seven different research teams are reviewed. Fundamental behaviors are ascertained from data. Measured strengths are compared with the current strength analysis method of the ACI Building Code. A new approach for strength analysis and design is developed and compared with the measured data.

Based on the analysis, the following conclusions are made:

1. Experimental data indicate no significant interaction between shear and normal moment applied to an edge connection at failure. Either the connection fails at its pure shear strength, or at its pure flexural strength, whichever is reached first.

2. The analysis model incorporated in the ACI Building Code (eccentric shear stress model) does not correlate well with measured edge connection strengths. On the average, it is excessively conservative and ratios of measured to predicted strengths are widely scattered.

3. Improved correlations between measured and calculated strengths can be obtained using the eccentric shear stress model if values of γ_v are reduced to values less than specified in the ACI Building Code.

4. An alternate strength analysis procedure is proposed. Consistent with trends of available experimental data, the procedure assumes no interaction between shear and moment. Shear strength is computed as the product between a critical section area and a critical shear stress capacity. Moment strength is computed as the flexural strength provided by reinforcement within an effective transfer width. Failure is calculated to occur when either of these is reached. The method is well suited for design and correlates well with the available test data.

ACKNOWLEDGMENTS

A research report by Alexander and Simmonds[2] shed light on most of the experimental data contained in this report. The analytical concepts presented in the earlier report inspired the analysis reported in the present paper. The research was funded partially by a grant from the National Science Foundation.

Additional funds were provided generously by the following: Robert Rosenwasser Associates, Rose Associates, S. and A. Concrete Co., Timko Contracting Corp., and Harry Macklowe Real Estate Co. — all located in New York, N.Y. Mete A. Sozen, professor of civil engineering at the University of Illinois at Urbana-Champaign, and J. W. Wallace and S.-J. Hwang, graduate research assistants at the University of California at Berkeley, provided valuable input to the substance and presentation of the paper. Findings reported in this paper are those of the author and do not necessarily represent the views of any of these organizations or individuals.

NOTATION

A_{cs} = cross-sectional area of slab critical section
c_t = transverse projection of torsional yield lines
c_1 = column dimension perpendicular to slab edge
c_2 = column dimension parallel to slab edge
d = d_{ave} = average effective depth of slab
d_t = slab effective depth for steel perpendicular to slab edge
f'_c = concrete compressive strength in psi
f_y = slab reinforcement yield stress
g = distance between centroids of column cross section and slab critical section
h = slab thickness
M_f = moment transfer strength limited by flexural strength of slab reinforcement placed within an effective transfer width
M_o = moment transfer strength in absence of shear transfer
M_c = ultimate moment transferred to connection at failure, measured at centroid of slab critical section
M_u = ultimate moment transferred to connection at failure, taken about column centroid
M_{cAD}, M_{cBC} = moment transfer strengths limited by shear stress capacity on faces AD and BC, respectively, of the slab critical section
N_d = force in diagonal compression strut
N_l = longitudinal component of force in diagonal compression strut
N_t = transverse component of force in diagonal compression strut
v_c = nominal shear stress capacity of slab
v_{AD} = shear stress computed on face AD of the slab critical section according to the eccentric shear stress model
v_{BC} = shear stress computed on face BC of the slab critical section according to the eccentric shear stress model
V_o = shear transfer strength in absence of moment transfer
V_u = ultimate shear transferred to connection at failure
α = angle between diagonal compression strut and slab edge
β_c = ratio of long to short side of column cross section
γ_v = proportion of transfer moment resisted by eccentric slab shear stress
ϕ = strength reduction factor
ρ = steel ratio of slab reinforcement within effective transfer width
ρ_b = balanced steel ratio
ρ_c = steel ratio of slab reinforcement at the column and perpendicular to the slab edge
ρ_l = steel ratio of slab reinforcement beyond the column and perpendicular to the slab edge
ρ_t = steel ratio of slab reinforcement parallel to the slab edge

REFERENCES

1. ACI Committee 318, "Building Code Requirements for Reinforced Concrete (ACI 318-83)," American Concrete Institute, Detroit, 1983, 111 pp.

2. Alexander, S. D. B., and Simmonds, S. H., "Shear-Moment Tranfer in Slab-Column Connections," *Structural Engineering Report* No. 141, Department of Civil Engineering, University of Alberta, Edmonton, July 1986, 95 pp.

3. Hanson, Norman W., and Hanson, John M., "Shear and Moment Transfer Between Concrete Slabs and Columns," *Journal,* PCA Research and Development Laboratories, V. 10, No. 1, Jan. 1968, pp. 2-16.

4. Hawkins, N. M.; Wong, C. F.; and Yang, C. H., "Slab-Edge Column Connections Transferring High Intensity Reversing Moments Normal to the Edge of the Slab," *Structures and Mechanics Report* No. SM 78-1, Department of Civil Engineering, University of Washington, Seattle, May 1978.

5. Kane, K. A., "Some Model Tests on the Punching Action of Reinforced Concrete Slabs at Edge Columns," Honours Project, The Queen's University of Belfast, 1978.

6. Regan, P. E., "Behavior of Reinforced Concrete Flat Slabs," *CIRIA Report* No. 89, Construction Industry Research and Information Association, London, 1981.

7. Scavuzzo, L., "Shear Reinforcement at Slab-Column Connections in a Reinforced Concrete Flat Plate Structure," The Royal Military College, Kingston, 1978.

8. Stamenković, A., and Chapman, J. C., "Local Strength at Column Heads in Flat Slabs Subjected to a Combined Vertical and Horizontal Loading," *Proceedings,* Institution of Civil Engineers (London), Part 2, V. 57, June 1974, pp. 205-232.

9. Zaghlool, E. R. F., "Strength and Behavior of Corner and Edge Column-Slab Connections in Reinforced Concrete Flat Plates," PhD thesis, Department of Civil Engineering, University of Calgary, 1971.

10. Masterson, D. M., and Long, A. E., "The Punching Strength of Slabs, A Flexural Approach Using Finite Elements," *Shear in Reinforced Concrete,* SP-42, American Concrete Institute, Detroit, 1974, pp. 747-768.

11. Zee, H. L., and Moehle, J. P., "Behavior of Interior and Exterior Flat Plate Connections Subjected to Inelastic Load Reversals," *Report* No. UCB/EERC-84/07, Earthquake Engineering Research Center, University of California, Berkeley, Aug. 1984, 130 pp.

12. Di Stasio, Joseph, Sr., and Van Buren, M. P., "Transfer of Bending Moment Between Flat Plate Floor and Column," ACI JOURNAL, *Proceedings* V. 57, No. 3, Sept. 1960, pp. 299-314.

13. ACI Committee 318, "Commentary on Building Code Requirements for Reinforced Concrete (ACI 318-83)," American Concrete Institute, Detroit, 1983, 155 pp.

14. Leet, Kenneth, *Reinforced Concrete Design,* McGraw-Hill Book Co., New York, 1982, 544 pp.

15. *CRSI Handbook,* 4th Edition, Concrete Reinforcing Steel Institute, Chicago, 1980, pp. 9-3 - 9-55.

16. Mitchell, Denis, and Collins, Michael P., "Diagonal Compression Field Theory—A Rational Model for Structural Concrete in Pure Torsion," ACI JOURNAL, *Proceedings* V. 71, No. 8, Aug. 1974, pp. 396-408.

17. Regan, P. E., and Braestrup, M. W., "Punching Shear in Reinforced Concrete: A State of the Art Report," *Bulletin d'Information* No. 168, Comité Euro-International du Béton, Lausanne, Jan. 1985, 232 pp.

18. Walker, P. R., and Regan, P. E., "Corner Column-Slab Connections in Concrete Flat Plates," *Journal of Structural Engineering,* ASCE, V. 113, No. 4, Apr. 1987, pp. 704-720.

19. Hawkins, Neil M., and Mitchell, Denis, "Progressive Collapse of Flat Plate Structures," ACI JOURNAL, *Proceedings* V. 76, No. 7, July 1979, pp. 775-808.